Relating Microhardness to Injection Molding Induced Morphology: A Study of Microbeam Synchrotron WAXD

Yutaka Kobayashi,[1,2] Hiroaki Kanno,[3] Yasuhiro Hanamoto,[3] Makoto Ando,[4] Toshitaka Kanai[2,4]

[1]*Research and Development Division, Prime Polymer Company, Limited, Sodegaura-City, Chiba 299-0265, Japan*
[2]*Division of Material Sciences, Graduate School of Natural Science and Technology, Kanazawa University, Kakuma-Machi, Kanazawa-City, Ishikawa 920-1192, Japan*
[3]*Analysis Research Laboratories, Mitsui Chemical Analysis and Consulting Service Incorporated, Sodegaura-City, Chiba 299-0265, Japan*
[4]*Performance Materials Laboratories, Idemitsu Kosan Company, Limited, Anasaki-Kaigan, Ichihara-City, Chiba 299-0193, Japan*

Received 7 April 2009; accepted 2 November 2009
DOI 10.1002/app.31719
Published online 5 January 2010 in Wiley InterScience (www.interscience.wiley.com).

ABSTRACT: The relationship between microhardness and morphology of polypropylene near the surface of injection molded plaques was investigated. Crystal structures and molecular orientation from the surface to shear oriented layer were characterized by microbeam synchrotron wide angle X-ray diffraction, polarizing optical microscope and Fourier transformed infrared spectroscopy. From precise measurements, using an X-ray beam with width of 0.35 μm, the frozen layer was divided into two layers. Molecular and crystal orientations changed greatly in the surface layer but remained constant in the inner layer. These oriented morphology did not affect microhardness along the depth direction on the cross-cut surface. Microhardness was proportional to crystallinity and showed a local maximum at shear oriented layer and a minimum at the surface. Then, positional dependence of microhardness was compared at the gate and the center of the plaque. Although crystallinity near the gate was lower than that at the center position, microhardness was higher. Therefore, crystallinity mainly affects microharness but superstructure like cross-hatching lamellae which is induced in biaxially extended melt flow is also not neglected in injection molded polypropylene parts. © 2010 Wiley Periodicals, Inc. J Appl Polym Sci 116: 1823–1831, 2010

Key words: hardness; injection molding; morphology; poly (propylene) (PP)

INTRODUCTION

Polypropylene (PP) is widely used in the automotive industry because it is lightweight, inexpensive, recyclable and easily processed by injection molding. The properties of PP are modified by adding fillers, elastomers and many kinds of additives to satisfy the required specifications for automotive parts, such as, bumper fascia, door panels, and dashboards. Recently the surface properties of injection molded PP have been becoming important for automotive parts because of environmental reasons. Better paintability of PP is required for the painting system from which volatile organic solvents are eliminated. In some cases painting itself is disused, therefore, better scratch resistance is an essential property for automotive parts. The area affecting the surface poperties is less than 20 μm of depth. There are few testing methods for mechanical properties in such small area except microhardness. Popular indentation hardness, measured for example by durometer, is not suitable for our experiment because its steel rod is around 1 mm of diameter. It is also difficult to measure crystal structure with the X-ray diffraction at the limited area of micron scale. The purpose of this article is to investigate the relationship between microhardness and injection molding induced morphology with using microbeam synchrotron wide angle X-ray diffraction (WAXD).

The morphology of injection molded PP is found to be a skin-core structure,[1] in which several layers were observed by polarizing optical microscope (POM). Layers are characterized by three to six structures from the surface to the core in an earlier study.[2] At present, the three layers related to the formation mechanism are usually discussed. Molten polymer in contact with the mold surface is frozen immediately and few spherulites appeared in this frozen layer. Shear flow inside the frozen layer is gradually cooled, and an oriented crystal structure which has high birefringence is observed in this shear oriented layer. The core layer contains spherulites because relaxation of flow history occurred during slow cooling in this region.[3] An X-ray scattering method has been applied to analyze crystal orientation of the skin-core structure. Molten polymer is

Correspondence to: Y. Kobayashi (y.kobayashi-@nifty.com).

subjected to large stress and a high deformation rate at the skin layer, so that c and a*-axis oriented lamellae occur at a high ratio compared to isotropic distributed ones. When wall thickness of a specimen is thin (1 mm), c-axis orientation ratio is higher than a* ratio at the skin layer.[4] Lamellae thickness, long period and crystallinity of injection molded PP specimens are measured from the surface toward the core by synchrotron SAXS. In the case of the specimen with a thickness of 1 mm, those three values are minimized at the core layer and maximized at the shear oriented layer. When the thickness increases, the depth profile of lamellae changes. A thick specimen of 5 mm shows maximum of lamellae thickness, long period and crystallinity at the core and minimum of them at the frozen layer.[5]

Differences in the crystal structure of polymers are related to microhardness which is measured by the instrumented microindentation method.[6] Microhardness on the surface of compression molded sheet is proportional to tensile modulus for several different PPs. And crystallinity measured by differential scanning calorimetry (DSC) is related to the properties.[7] In the case of injection molded PP, microhardness on the cross-cut surface indicates the local maximum at the shear oriented layer and the minimum at the skin layer. Crystallinity near the surface is considered to be small from the result.[8] For linear low density polyethylene, increasing comonomer in polyethylene leads to a decrease in the thickness of crystalline lamellae and in crystallinity at the same time. Both crystal factors are proportional to microhardness in this case.[9] Large deformation rate and quenching in injection molding affect not only crystallinity but also crystal size and polymorphism of polymers. Although α-form crystal of PP (density 936 kg/m^3) is changed in its mesomorphic form (880 kg/m^3) by rapid cooling in quiescent crystallization, microhardness is only related to the density of PP.[10] The effect of lamellar size on microhardness is not clear. At least the lower microhardness is observed on the stacking lamellar structure in which amorphous region between lamellae is large.[11]

Although a lot of previous studies have looked at skin structure in injection molded PP, there were few observations of WAXD at the 1 μm^2 area along the normal direction of the cross-cut surface. We focus on the relationship between microhardness and the morphology. Improving surface properties is important for industrial applications of PP. Our aim in this work is to analyze the crystal structure close to the surface in injection molded PP and to clarify factors which affect to microhardness near the surface. The experimental methods for evaluating molecular orientation were Fourier transformed infra-red spectroscopy (FTIR) and birefringence with POM. Crystal structure at the skin was analyzed by microbeam synchrotron WAXD. The depth profile of microhardness was measured by instrumented microindenter with a Vickers pyramid diamond and a Knoop rhombic-based pyramid diamond.

EXPERIMENTAL

Material and molding conditions

Characteristics of PP used in this study were Ziegler–Natta isotactic homopolymer (MFR 13 g/10 min for 2.16 kg at 230°C, pentad ratio 97%), molecular weight (M_w 306 kg/mol, M_w/M_n 8.3) and nucleating agent was added. Rectangular plaques ($^w70 \times {}^l270 \times {}^t3$ mm) were molded by using an injection-molding machine, Toshiba IS100F-III. The molding conditions were as follows; mold temperature 40°C, barrel temperature 200°C, filling time 3 s, holding time 8 s and curing time 20 s. Injection pressure was controlled automatically to keep constant injection velocity. Compression molded plaques ($^w150 \times {}^l150 \times {}^t3$ mm) were prepared for comparison of flow history. Pellets were molten between aluminum plates at 200°C for 5 min, then pressed for 2 min, and finally cooled rapidly to 20°C.

Microhardness measurements

Microhardness was measured using an Elionix ENT-1100a tester at room temperature. A Vickers and a Knoop indenter tips were used for the experiment and microhardness data using these indenter tips were given by H_V and H_K, respectively (Fig. 1). The hardness values based on H_V and H_K are not directly comparable. The Vickers hardness is calculated by the contact area, whereas the Knoop hardness is

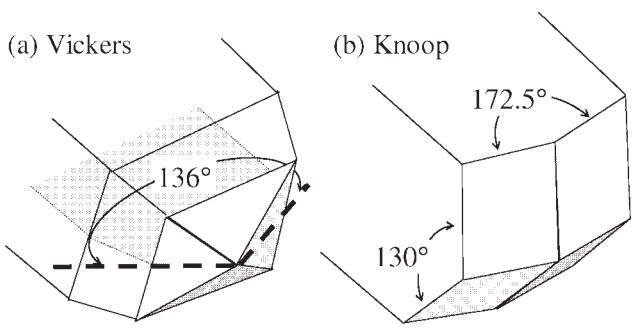

$$H_V = \frac{F}{A_{surface}} = \frac{F}{26.43h^2} \qquad H_K = \frac{F}{A_{projected}} = \frac{F}{65.44h^2}$$

Figure 1 Geometries of two indenters. Microhardness for a Vickers and a Knoop indenters are given by H_V and H_K respectively. F; applied force, A; contact area and h; indentation depth.

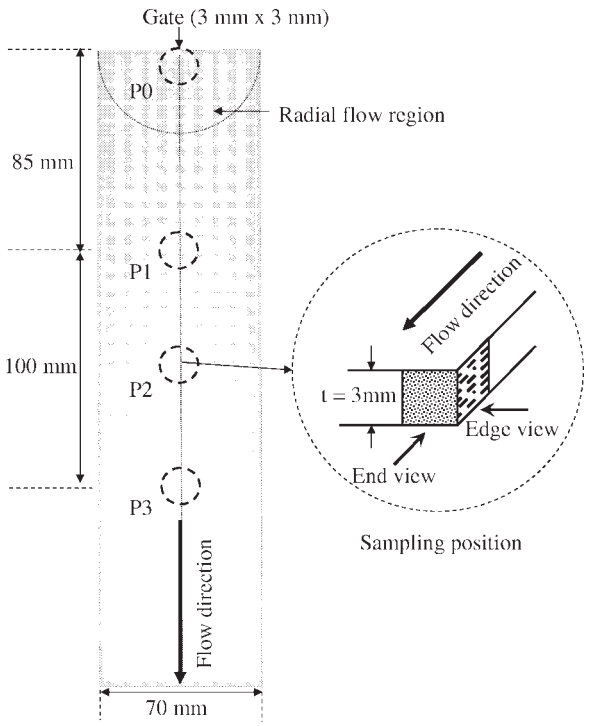

Figure 2 A schematic diagram of an injection molded plaque and specimens cut at the distance of 5, 85, 135, and 185 mm away from the gate.

based on the projected area. Studied positions for injection molded plaques were located 5 mm (P0) and 135 mm (P2) from the gate, close to the center of the part (Fig. 2). These distances were measured between the gate and the marking on the wall of the cavity. For compression molded specimens, the center position was studied. Measurements were performed on the surface of molded plaques and the cross-cut surface parallel to the flow direction (edge view). The cross-cut surface was polished by a Buehler Ecomet 3000 apparatus with 0.05 μm alumina paste. To evaluate anisotropy of the specimens, the long diagonal of the Knoop indenter was applied to the flow direction (FD) and the perpendicular direction, more specifically, the transverse direction (TD) on the molded surface and the normal direction (ND) on the cross-cut surface. All data were measured five times, and then average and standard deviation were calculated for clarifying the precision of the hardness. The standard deviations on H_V were 1.26 at P0 and 0.54 at P2, respectively.

Morphological characterization

The molded specimens were characterized by three types of experimental techniques; polarizing optical microscope (POM), microbeam synchrotron wide angle X-ray diffraction (WAXD) and Fourier transform infrared spectroscopy (FTIR). The POM observation was carried out using Olympus BH-2 with a Berek compensator at room temperature. Studied positions were located 5 mm (P0), 85 mm (P2), 135 mm (P3), and 185 mm (P4) from the gate (Fig. 2). Morphology of the microtomed section was viewed parallel to the flow direction (edge view).

The WAXD experiment was carried out using synchrotron radiation at the beam line, BL24XU of SPring-8 at Japan Synchrotron Radiation Research Institute (JASRI). The instrument used a light collection optical system with zone plates and a detector system with image plates (Rigaku R-AXIS). The square-shaped microbeam had a dimension of 0.35 μm × 1.5 μm and a wavelength of 1.2398 Å (10 keV). The PP specimens were mounted at 86.81 mm from the image plate. The studied positions in the molded plaques were located at P0 and P2. Measurements were performed at room temperature with the microbeam being along the flow direction (end view) and from the surface to the core along a normal direction in the specimens. All X-ray data were corrected for background (air and instrument) scattering before analysis. Precision of crystallinity was estimated ±1.5%, because differences in a thickness of the specimen and the measured position affected the results in a microbeam synchrotron X-ray method.

The FTIR experiment was carried out with a Nicolet 8700 and Continuum microscope at room temperature. The equipment was operated in transmission mode with 100 scans per sampling at a resolution of 1 cm^{-1} in the wavenumber range between 4000 and 650 cm^{-1}. Observed positions in the specimen were the same as those for the WAXD experiment. The microtomed cross-cut section of the specimen, 40 μm thickness, was measured with an aperture size of 30 μm × 150 μm in the normal direction. All spectra were collected for background spectra to remove the atmospheric effects such as carbon dioxide and the moisture in the air.

RESULTS

Microhardness with Vickers indenter

Ziegler–Natta isotactic PP specimens prepared by an injection molding and a compression molding were compared using a microindentation method. Microhardness (H_V) at the P2 position was measured in the normal direction at 200 μm intervals with the Vickers indenter (Fig. 3). The indentation depth was varied from 1.7 μm to 2.2 μm by the applied load of 10 mN. The length of the diagonal of the residual impression was around 9.8 μm. Because the zone of plastic deformation under the indenter is about 4–5 times the indentation depth,[12] measured values mainly depend on the crystal structure of 10 μm thickness below the surface. Microhardness for

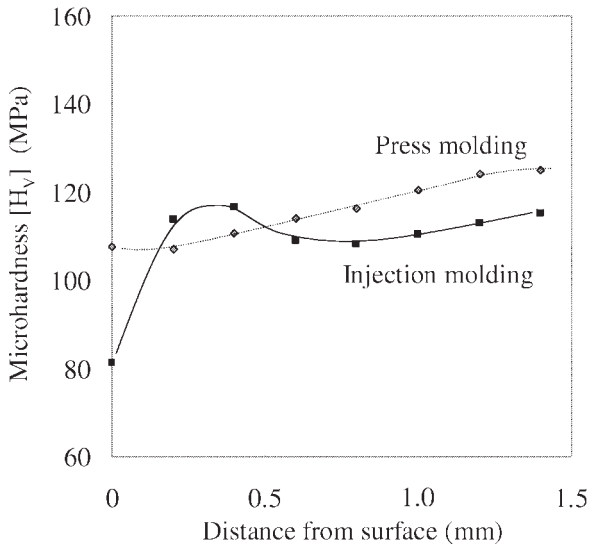

Figure 3 The microhardness (H_V) profile from the surface to the core at the position P2 of injection molded plaque and compression molded one. Measurement conditions: indentation load 10 mN, room temperature.

injection molded PP shows the local maximum at 0.2–0.4 mm depth and the minimum on the surface. It is technically important that microhardness on the surface is obviously small in injection molded PP, compared with compression molded one. The profile near the surface in injection molded PP has already been reported and considered to have occurred by low crystallinity.[8] Although the shapes of H_V depth profile near the surface at the P0 and P2 positions are similar, the absolute value of H_V at P0 position was higher than that at the P2 position (Fig. 4). This difference between the H_V values at the gate and at

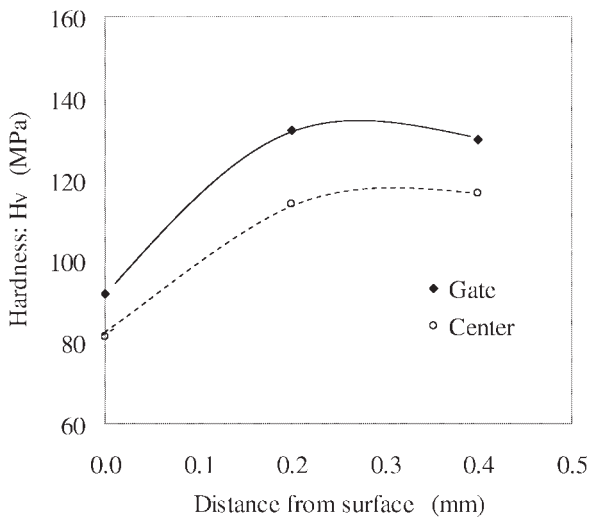

Figure 4 Microhardness (H_V) near the surface at the position P0 (gate) and P2 (center) of injection molded plaque. Measurement conditions: indentation load 10 mN, room temperature.

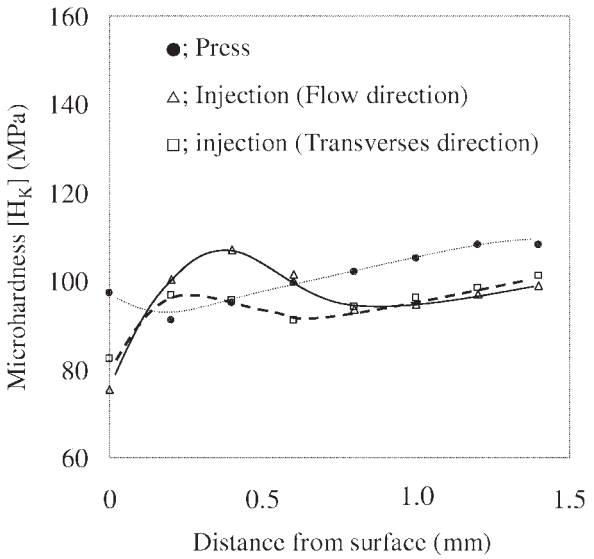

Figure 5 The Microhardness (H_K) profile from the surface to the core at the position P2 of injection molded plaque and compression molded one. The long diagonal of Knoop indenters are applied parallel and perpendicular to the flow direction. Measurement conditions: indentation load 30 mN, room temperature.

the other positions in the same plaque has not been studied extensively before this work.

Microhardness with Knoop indenter

A Knoop indenter is suitable for evaluating anisotropy of microhardness because of the rhombic-based tip compared to a square-based one. The depth profile of the microhardness (H_K) at P2 position was measured by setting the long diagonal of Knoop indenter parallel and perpendicular to the flow direction (Fig. 5). Indentation depth was around 2.0 μm by the applied load of 30 mN. Lengths of long and short diagonal residual impressions were around 61 μm and 8.6 μm, respectively. Therefore, the measured area for H_K is 4 times larger than that for H_V. Higher H_K in the flow direction was observed in the range of 0.2–0.6 mm depth. Crystal orientation is related to the anisotropy of microhardness. The microhardness of the transcrystalline layer is higher by up to 30% when the longer diagonal of the Knoop tip is perpendicular to the transcrystalline growth direction, compared to when the diagonal is parallel to that direction.[13] Less H_K anisotropy was detected for the compression molded specimen.

Birefringence using POM

Birefringence of the cross-cut section at the P2 position from the edge view shows a typical V-pattern,[14,15] sharp dropping at the frozen layer and increasing at the shear oriented layer (Fig. 6). The

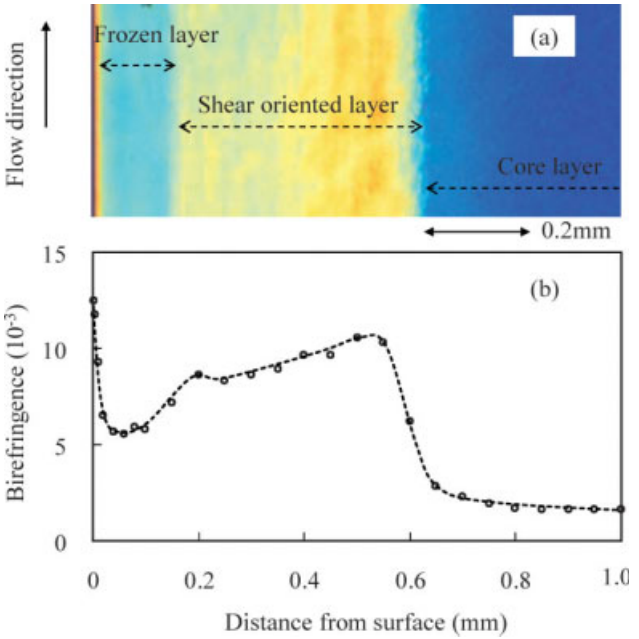

Figure 6 Morphology of the cross-cut section observed by POM in the P2 position. (a) Micrograph along the flow direction with the specimen rotated by 45 degrees from the direction of polarizer. (b) Birefringence to the depth direction. [Color figure can be viewed in the online issue, which is available at www.interscience.wiley.com.]

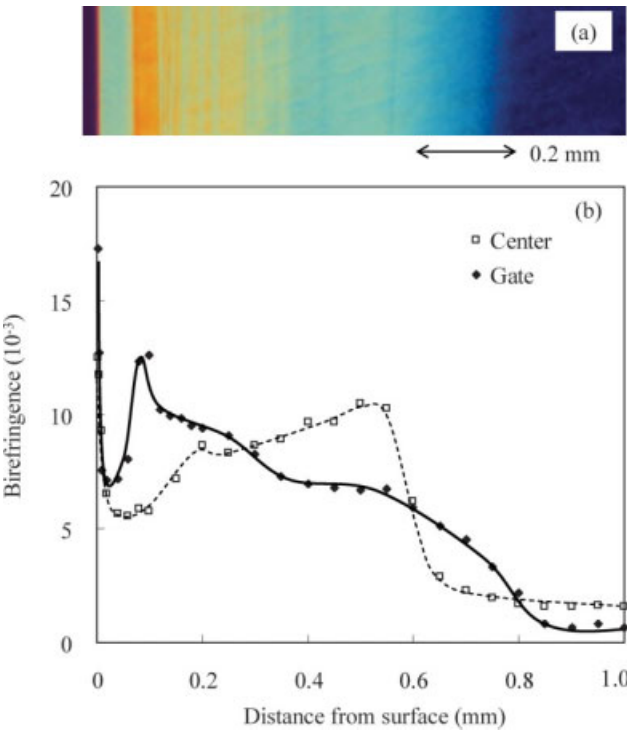

Figure 7 Morphology of the cross-cut section observed by POM in the P0 position. (a) Micrograph along the flow direction with the specimen rotated by 45 degrees from the direction of polarizer. (b) Birefringence along the normal direction comparing P0 and P2 position. [Color figure can be viewed in the online issue, which is available at www.interscience.wiley.com.]

measurement was also carried out at P0, P1, and P3 positions in the same way. Although the V-patterns at the P1-P3 positions were similar, birefringence at P0 was higher than those at the other positions and showed a sharp peak (Fig. 7). For uniaxially oriented semicrystalline polymers, the measured birefringence was analyzed by a two phase model of crystalline and noncrystalline.[16] Intrinsic birefringences of perfectly oriented crystalline and noncrystalline PPs were 0.023–0.030 and 0.060–0.086, respectively.[17] Therefore, the amorphous region has stronger affects on the observed birefringence when the volume fractions and orientation functions of crystalline regions and noncrystalline are equivalent, respectively.

Crystal structure using microbeam synchrotron WAXD

The WAXD patterns of injection molded PP at 0.3 mm depth in the P0 and P2 positions were obtained under the conditions of the end view, 0.35 μm × 1.5 μm beam dimension and room temperature (Fig. 8). These reflections are indexed as the (110), (040), (130), (111), (131), and (041) of α-form crystal of PP. The presence of β-form crystal (300) was detected for the specimen taken at the P2. The relationship between those WAXD patterns and orientations of c-axis and b-axis of monoclinic crystal is well known.[18] According to this, we used the relative intensity, (110)/[(111) + (131) + (041)], as an

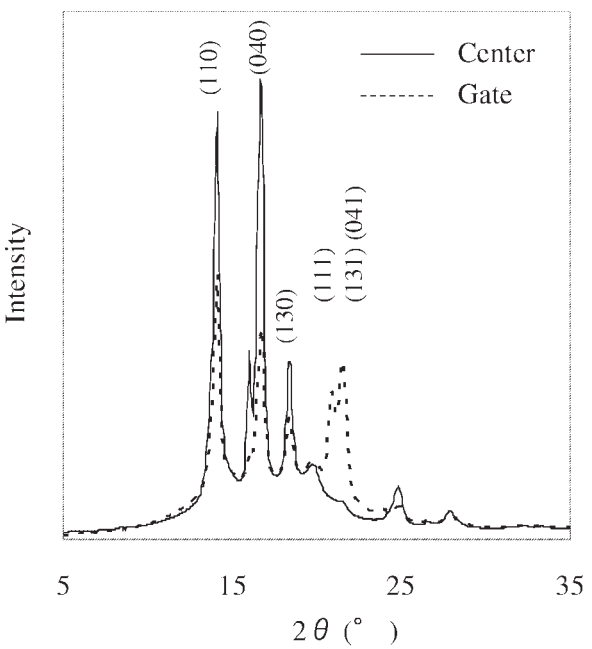

Figure 8 Comparison of WAXD patterns measured at 0.3 mm depth of cross-cut section in the P0 (gate) and P2 (center) positions. Conditions; the end view, beam dimension 0.35 μm × 1.5 μm, room temperature.

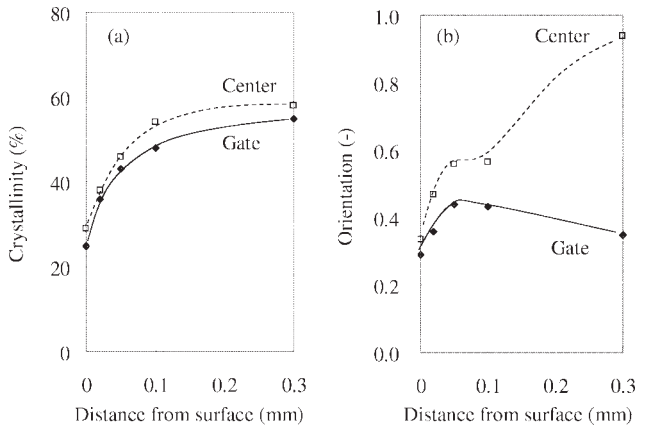

Figure 9 Changes in crystal structure, (a) crystallinity and (b) orientation, from the surface to 0.3 mm depth at the P0 (gate) and P2 (center) positions. Conditions; end view, beam dimension 0.35 μm × 1.5 μm, room temperature.

index of the crystal orientation to the flow direction in this study. Figure 9 shows changes in crystal structures from the surface to 0.3 mm depth at the P0 and P2 positions. Although crystallinities in those positions were increasing along the depth direction, crystal orientation at the P0 changed less than that at the P2 position. Crystallinity and crystal orientation in the frozen layer for injection molded plaques are generally lower than that in the shear oriented layer,[4,5] because molten PP is quenched on the cold wall of a mold tool. At the same time, the shear oriented layer has higher crystalllinity and orientation compared with the core layer, because a large shear rate induces crystallization of PP during an injection molding process. The lower crystallinity and orientation at the P0 position despite a high shear rate were investigated from another point of view using FTIR.

Crystal structure using FTIR

The FTIR spectra were often used to determine crystallinity of PP based on the relative absorbance of A997/A973 and A841/A973.[19] It is opposite to the results from X-ray scattering methods[4,5] that the FTIR method leads to the decreasing of crystallinity at the shear oriented layer for the depth profile.[20] Recently, the IR bands at 973, 998, 841, and 1220 cm^{-1} correspond to helical structures with the minimum n values 5, 10, 12, and 14 monomer units in helical sequences, respectively.[21,22] Figure 10 shows changes in the relative absorbance of A998/A973 and A841/A973 measured from the surface to the core at 0.2 mm intervals at the P0 (gate) and P2 (center) positions. The depth profile of A998/A973 in the P2 position was upside down to that of the birefringence. Therefore, long helical sequences (minimum $n = 12$) are reduced in the shear oriented region. This phenomenon is supported by the small relative absorbance at P0 where high birefringence was observed. The reason is discussed in the next section.

DISCUSSION

Crystal structure near the surface

The essential difference between the results in the earlier works[4,5] and those in the present work is the analyzing area. To focus on characterizing the frozen layer of injection molded PP, we measured using an X-ray beam with a width of 0.35 μm. The previous measured crystal structure was averaged to the depth direction, because of the microtomed thickness of 35 μm[4] or the microbeam of 200 μm width.[5] The thickness of the frozen layer was around 130 μm in the injection molded plaque except for the radial flow area (Figs. 2 and 6), so that it had been difficult to measure the depth profile of crystal in a frozen layer.

Firstly, the crystal structure close to the surface at the P2 position will be discussed on fountain flow concept.[15] The frozen layer is structurally divided into two regions, (A) 0–0.04 mm and (B) 0.04−0.13 mm (Fig. 11). In the region A, birefringence is sharply decreasing, on the other hand, crystallinity and crystal orientation are increasing. Molten PP subjected to large elongational stress in the flow front contacts with the mold surface, and then, is frozen along the depth direction. Therefore, large molecular orientation to the flow direction and the

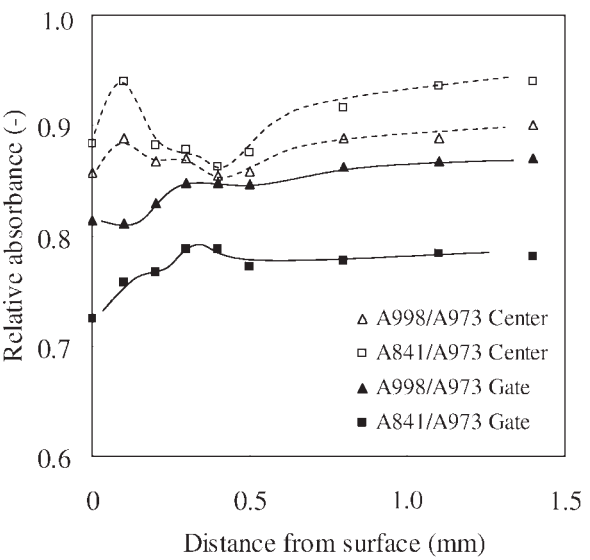

Figure 10 Changes in the relative absorbance of the IR spectra related to monomer units in helical sequences of PP. Measured position; from the surface to the core at 0.2 mm intervals in the P0 (gate) and P2 (center) positions. Conditions; edge view, aperture size of 30 μm × 150 μm, room temperature.

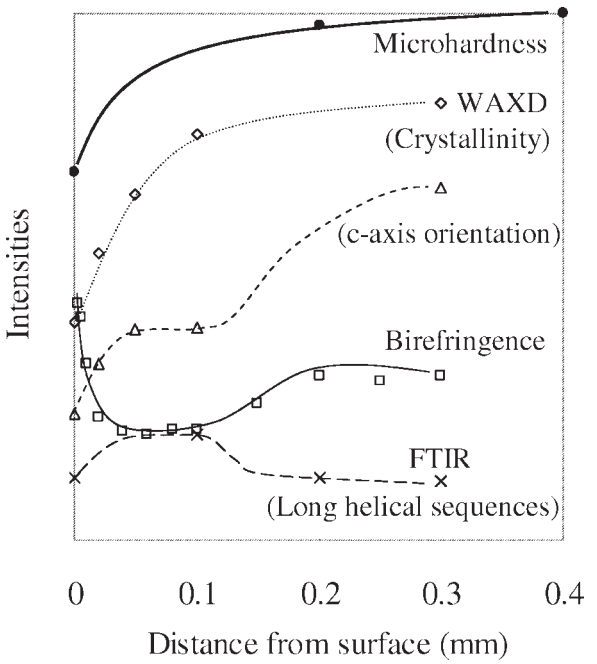

Figure 11 Overwritten graph of WAXD, POM and FTIR data along the normal direction at P2 position of the injection molded plaque. Original graphs; Figure 3 for microhardness, Figure 9 for WAXD, Figure 6 for birefringence and Figure 10 for FTIR.

disordered α-form crystal are observed at the surface. The mesomorphic form crystal is expected for the high cooling rates at the surface.[23] The relaxation process of stretched polymer chains takes place below the surface and crystallinity and crystal orientation are increasing at the same time. In the region B, birefringence and crystal orientation stay constant despite increasing crystallinity. Delay of cooling below the surface increases the time for crystallization of PP. Crystal and molecular orientations are controlled by anisotropy of stress. As mentioned in the region A, extensional deformation is gradually relaxed toward depth direction. At the same time, molten PP is subjected to shear deformation. We consider two possible causes for the constant birefringence and crystal orientation. (a) Reducing elongational stress and increasing shear stress for the orientations are balancing in the region B. (b) Because birefringence of a crystal portion is affected by crystal orientation and crystallinity, observed constant birefringence means that decreasing molecular orientation and increasing amount of the oriented crystal is balancing in region B. Further studies will be required to fully understand this mechanism.

Secondly, the crystal structure near the gate is discussed. Lots of earlier works have suggested that cross-hatch or shish-kebab like structure is formed at the skin layer in injection molded PP.[1,5] These superstructures have been measured at the position far from the gate, where molten polymer is deformed two dimensionally within MD-ND plane. Although crystal orientation in the flow direction in Figure 9(b) is well-known at the shear oriented layer,[18] there is little orientation at the P0 position. Molten polymer flowing into the cavity through the gate is stretched biaxially in the direction of thickness and width (Fig. 12) and the high stress remains by the flow with a high deformation rate. The relative amount of long (A841/A973) and short (A998/A973) helical sequences along the depth direction at the P0 position is opposite at the P2 position in Figure 10. Consequently lower crystallinity near the gate is caused by less crystal perfection and crystal structures are found not to be stacking lamellae which are ordering to the flow direction, but one with some biaxial nature.

Microhardness and morphology

Among the conventional polymers PP has poor scratch resistance compared to amorphous polymers with a high glass transition temperature. Improving surface hardness is important for industrial applications of PP, therefore, we try to clarify factors which affect to microhardness near the surface. Although the strong molecular orientation occurred near the surface in the P2 position, the hardness (H_V) value was smaller than that of the compression molded plaque. Earlier report suggests that crystallinity decreases toward the surface whose cause is quenching on the mold wall.[8] The depth profiles of the microhardness are explained with respect to crystallinity in this experiment, and we have confirmed the higher microhardness near the gate (P0 position) despite lower crystallinity. Reduced free amorphous

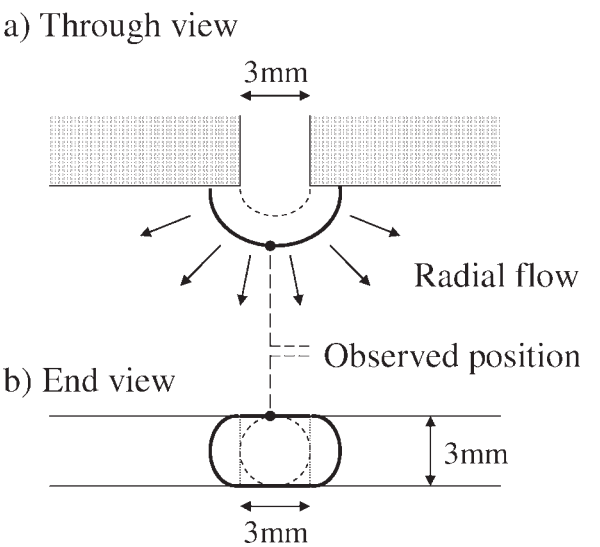

Figure 12 A schematic diagram of radial flow near the gate (P0 position) in an injection molded plaque.

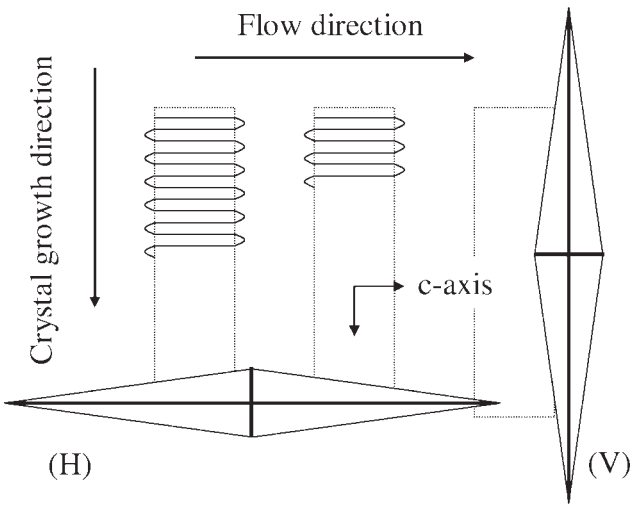

Figure 13 The relationship between crystal growth direction and the long diagonal of Knoop indenter for uniaxially oriented crystal structure; (H) parallel to the flow direction, (V) perpendicular to the flow direction.

fraction by biaxially stretching is one possible cause for this result. Although helical sequences are more than 12 monomer units smaller at the P0 than at the P2 (Fig. 10), there are less difference in the mesomorphic phase between these positions (Fig. 8). In the case of crystallization under the quiescent conditions, quenching rate up to 1000°C/sec is linearly related to density and microhardness of PP and α-form crystal changed to mesomorphic phase during the rapid cooling process.[10] The work suggests that microhardess is proportional to crystallinity even if rigid amorphous fraction is increased by the restriction of mobility of free amorphous on the surfaces of tiny crystallites.[24] Therefore, lamellar structures induced by biaxial flow are more important than rigid amorphous for scratch resistance.

From the experiment with the Knoop indenter, the hardness (H_K) became lower when the long diagonal of the indenter is applied parallel to the crystal growth direction.[13] In an injection molded plaque, lamellae are arranged randomly in the core layer and perpendicular to the flow direction in the skin layer.[25] Because the inter lamellar (amorphous) layer deforms more easily than lamella itself by stress, the long diagonal direction greatly affects the deformation of uniaxially oriented crystal structure (Figs. 5 and 13). In addition, residual stress in a specimen does not increase microhardness.[26] Yield strength corresponded of the disruption of lamella continuity and a higher force is required for the disruption to the cross-hatched structure because of higher density of active lamellar pulling points.[27] A higher ratio of tangential lamellae increase yield energy, so the yielding process is basically governed by the superstructure.[28] Therefore, crystallinity mainly affected to microhardness but superstructure like cross-hatched lamellae which is induced biaxially in extended melt flow is also not neglected in the injection molded PP plaques.

CONCLUSION

This study discusses the relationship between microhardness and morphology at the surface of the injection molded PP plaques. To measure the properties at a micron scale, the instrumented microindentation and microbeam synchrotron WAXD were used into the experiment. Although many earlier works characterized the frozen layer, the crystal structures were averaged by thickness of the specimens or limit of aperture size of the analytical instruments. In this research the crystal structure along the depth direction on the cross-cut surface of the specimen was measured by using an X-ray beam with a width of 0.35 μm.

Two distinct structures were observed in the frozen layer. At the surface region, molecular and crystal orientations were changed sharply. At the inner region, the structures stayed constant. Morphology did not affect microhardness along the depth direction on the cross-cut surface, but crystallinity was proportional to the hardness. From a comparison of microhardnesses at the gate and the center positions in the molded plaque, microhardness near the gate was larger despite lower crystallinity.

The microhardness, which is very important for automobile parts, is very much influenced by crystallinity. In case of multi-extentional flow near the gate, the microhardness is influenced by not only crystallinity but also by biaxially extended orientation which easily forms a superstructure like cross-hatched lamellae.

A part of this work was performed at the beam-line BL24XU of SPring-8 at Japan Synchrotron Radiation Research Institute (JASRI). The project number was 2008A3209.

References

1. Fujiyama, M. Polypropylene; Karger-Kocsis, J., Ed. Chapman and Hall: London, 1995; Vol. 1, 167–204.
2. Kantz, M. R.; Newman, H. D., Jr.; Stigale, F. H. J Appl Polym Sci 1972, 16, 1249.
3. Michael, R. A.; Wolkowicz, D. Polypropylene Handbook, 2nd ed.; Pasquini, N., Ed. Carl Hanser Verlag: Munich, 2005; 238–241.
4. Mendoza, R.; Régnier, G.; Seiler, W.; Lebrun, J. L. Polymer 2003, 44, 3363.
5. Zhu, P.; Edward, G. Polymer 2004, 45, 2603.
6. Baltá Calleja, F. J TRIP 1994, 2, 419.
7. Arranz-André, J.; Penã, B.; Benavente, R.; Pérez, E.; Cerrada, M. L. Eur Polym J 2007, 43, 2357.
8. Aurrekoetxea, J.; Sarrionandia, M. A.; Urrutibeascoa, I.; Maspoch, M. L. I. Polymer 2003, 44, 6959.

9. Fakirov, S.; Krumova, M.; Rueda, D. R. Polymer 2000, 41, 3047.
10. Tranchida, D.; Piccarolo, S. Polymer 2005, 46, 4032.
11. Koch, T.; Seidler, S.; Halwax, E.; Bernstorff, S. J Mater Sci 2007, 42, 5318.
12. Baltá Calleja, F. J.; Fakirov, S. Microhardness of Polymers; Cambridge University Press: Cambridge, 2000; p 13.
13. Amitary–Sadovsky, E. D. J Polym Sci B: Polym Phys 1999, 37, 523.
14. Kamal, M. R.; Tan, V. Polym Eng Sci 1979, 19, 558.
15. Tadmor, Z. J Appl Polym Sci 1974, 18, 1753.
16. Samuels, R. J. Structured Polymer Properties; Wiley-interscience: New York, 1974; pp 51–63.
17. Seferis, J. C. Polymer Handbook, 4th ed.; Brandrup, J.; Immergut, E. H.; Grulke, E. A., Eds.; Wiley-interscience: New York, 1999; Chapter 6, p 571.
18. Zipper, P.; Janosi, A.; Geymayer, W.; Ingolic, E.; Fleischmann, E. Polym Eng Sci 1996, 36, 467.
19. Law, A.; Simon, L.; Lee-Sullivan, P. Polym Eng Sci 2008, 48, 627.
20. Trotignon, J. P.; Verdu, J. J Appl Polym Sci 1990, 39, 1215.
21. Zhu, X. Y.; Yan, D. Y.; Fang, Y. P. J Phys Chem B 2001, 105, 12461.
22. An, H.; Zhao, B.; Ma, Z.; Shao, C.; Wang, X.; Fang, Y.; Li, L.; Li, Z. Macromolecules 2007, 40, 4740.
23. Pantani, R.; Coccorullo, I.; Speranza, V.; Titomanlio, G. Prog Polym Sci 2005, 30, 1185.
24. Zia, Q.; Mileva, D.; Androsch, R. Macromolecules 2008, 41, 8095.
25. Naiki, M.; Fukui, Y.; Matsumura, T.; Nomura, T.; Matsuda, M. J Appl Polym Sci 2001, 79, 1693.
26. Anthony, C. Fischer-Cripps. Nanoindentation; Springer-Verlag: New York, 2002; pp 20–35.
27. Viana, J. C. Polymer 2005, 46, 11773.
28. Nitta, K.; Yamamoto, Y. e-Polymers 2003. Available at http//www.e-polymers.org.